

Constraints On Dark Energy Models From Galaxy Clusters and Gravitational Lensing Data

Alexander Bonilla^{1,*} and Jairo E. Castillo^{2,†}

¹*Departamento de Física, Universidade Federal de Juiz de Fora, 36036-330, Juiz de Fora, MG, Brazil*

²*Facultad Tecnológica, Unversidad Distrital Francisco José de Caldas, Carrera 7 No. 40B - 53, Bogotá, Colombia*

The Sunyaev-Zeldovich (SZ) effect is a global distortion of Cosmic Microwave Background (CMB) spectrum as result of its interaction with a hot electron plasma in the intracluster medium of large structures gravitationally viralized such as galaxy clusters (GC). Furthermore, this hot gas of electrons emits X-Rays due to its fall in the gravitational potential well of the GC. The analysis of SZ and X-Ray data, provide a method for calculating distances to GC at high redshifts. On the other hand, many galaxies and GC produce a Strong Gravitational Lens (SGL) effect, which has become a useful astrophysical tool for cosmology. We use these cosmological tests in addition to more traditional ones to constrain some alternative dark energy models, including the study the history of expansion through the cosmographic parameters. Using Akaike and Bayesian Information Criterion we find that the w CDM and Λ CDM models are the most favoured by the observational data. In addition, we found that at low redshift appears a peculiar behavior of slowdown, which occurs in some dynamical dark energy models using data only from GC.

PACS numbers: 98.80.-k; 98.80.Es

I. INTRODUCTION

Several authors have used the SZ effect, X-rays and SGL data from galaxies and GC to provide independent estimations of cosmological parameters. The combination of X-rays and the SZ data lead to two useful cosmological tests namely, angular diameter distance d_A [1] and gas mass fraction f_{gas} of the GC [2]. Both tests have been used in the literature to investigate dark energy [3] and modified gravity ([4] and reference therein). Additionally, the SGL observations also can be used to probe the dark matter and dark energy properties [3]. Therefore, to use the GC measures constitutes an independent and complementary test to probe cosmological models. Now, from the phenomenological point of view the Λ CDM model is the most accepted to date, which predicts that the universe consists of approximately 4% of baryonic matter, 26% of Cold Dark Matter (CDM) and about 70% is a exotic component known as dark energy (DE) which is the main responsible for the accelerated expansion of the Universe. In the concordance model (Λ CDM), the CDM is made up of collisionless non baryonic particles and the DE is provided by the cosmological constant Λ with an equation of state (EoS) $w = -1$. This model is in excellent agreement with the observations of the CMB radiation, baryonic acoustic oscillations (BAO) and Supernova Ia (SNIa). Nevertheless, the standard model has some fundamental problems related to the nature of the dark matter and dark energy [5, 6]. In the context of DE, there are several theoretical arguments against a cosmological constant. One is the coincidence problem, that is, why today the value of dark energy density is of the same order of magnitude than dark matter density. Another important fundamental issue is the fine tuning of the present value of Λ which is completely in disagreement with the predictions of particle physics [7, 8]. Therefore, several dark energy models with a dynamical EoS have been proposed to alleviate the problems of the cosmological constant [6].

Our main aim in this paper is to improve and update the constraints on some well established cosmological models in the literature with the use of GC and SGL in the frame of Friedmann-Lemaître-Robertson-Walker ($FLRW$) universe.

This paper is organized as follows. The next section (§ II) we introduce the cosmological tests and the statistical analysis. In § III we describe cosmological models of dark energy, including the main results. The history of expansion is analyzed in § IV. In section § V we conclude with the summary and the discussion.

*Electronic address: abonilla@fisica.ufjf.br

†Electronic address: jecastillo@distrital.edu.co

II. GALAXY CLUSTERS

A. Angular diameter distance using SZ/X-Ray method

The thermal SZ effect is a small distortion in cosmic microwave background (CMB) spectrum due to the inverse Compton scattering of the CMB photons when they pass through the hot gas of electrons in GC [10, 11]. This small fluctuation in CMB temperature is characterized by $\Delta T_{sz}/T_{cmb} = f(\nu, T_e)y(n_e, T_e)$, where

$$y(n_e, T_e) = \int_{los} n_e \frac{k_B T_e}{m_e c^2} \sigma_T dl, \quad (1)$$

which is known as the Compton parameter, such that $T_{cmb} = 2.726K$, n_e and T_e are the temperature of CMB, electron number density and temperature of the hot gas respectively. σ_T is the Thomson cross section, k_B is the Boltzmann constant, $m_e c^2$ is the rest mass of the electron and the integration is along the line of sight (*los*). The dependence with the frequency of the thermal SZ effect is given through the term $f(\nu, T_e)$, which also introduces relativistic corrections (see for [12] more details).

On the other hand, gas in GC can reach temperatures of $10^7 - 10^8 K$ and densities of the order of $10^{-1} - 10^{-5} cm^{-3}$, so they emit high amounts of energy in X-Ray. The primary emission mechanisms of X-Ray for a diffuse intra-cluster medium are collisional processes such as: free-free (Bremsstrahlung), free-bound (recombination) or bound-bound (mainly emission lines), with luminosities of the order of $10^{44} erg/s$ or even higher and spatial extensions of several arcmin or larger, even at high redshift. X-Ray's observations currently offer a powerful technique for building catalogs of galaxy clusters, which are very important for modern cosmology [13]. The X-ray GC emission is given by

$$S_x = \frac{1}{4\pi(1+z)^4} \int n_e^2 \Lambda_{eH}(\mu_e/\mu_H) dl, \quad (2)$$

where Λ_{eH} is the X-ray cooling function, μ is the molecular weight given by $\mu_i = \rho/(n_i m_p)$ and z is the cluster redshift [1, 2]. Then, combining equations 1 and 2 through n_e we can obtain experimental cosmological distance with triaxial symmetry, given by

$$D_{c|exp}^{ell} = \frac{\Delta T_{sz0}^2}{S_{x0}} \left(\frac{m_e c^2}{k_B T_e} \right)^2 \frac{g(\beta)}{g(\beta/2)^2 \theta_{c,proj}} \frac{\Lambda_{eH}(\mu_e/\mu_H)}{4\pi^{3/2} f(\nu, T_e)^2 T_{cmb}^2 \sigma_T^2 (1+z)^4}, \quad (3)$$

where ΔT_{sz0} and S_{x0} are the central temperature decrement and the central surface brightness respectively, which includes all the physical constants and the terms resulting from the *los* integration, such that $\Delta T_{sz0} \propto d_A(z)$, $S_{x0} \propto d_A(x)$ and $d_A(z) = D_{c|exp}^{ell} h^{3/4} (e_{proj}/e_1 e_2)^{1/2}$, h is a function of GC shape and orientation, e_{proj} is axial ratio of the major to minor axes of the observed projected isophotes and $\theta_{c,proj}$ is the projection on the plane of the sky (*pos*) (see Appendix A for some useful relationships and Table VIII for some data used in these method). The expression in Eq. 3 is a observational quantity that depends basically of the physical and geometrical properties of the cluster (see [1] for more information about the astrophysical details). That method for measuring distances is completely independent of other techniques and is valid at any redshift. We use 25 measurements of angular diameter distances from GC obtained through SZ/X-Ray method by De Filippis et al. (see Fig. 5.). In our analysis, we follow the standard procedure and minimize the χ^2 function

$$\chi_{dis}^2(z_i, \Theta) = \sum_{i=1}^{25} \frac{(D_{c|exp}^{ell}(z_i) - d_A(z))^2}{\sigma_{D_c}^2}, \quad (4)$$

where $d_A(z)$ is the angular diameter distance in a *FLRW* universe and $\sigma_{D_c}^2$ are the errors associated with $D_{c|exp}^{ell}(z_i)$ (see Table VIII in Appendix).

B. The gas mass fraction f_{gas}

Another independent cosmological technique is to derive d_A using the gas mass fraction data from GC. In order to use f_{gas} as cosmological test we need to assume that there is a proportion between the baryonic fraction of the GC

and the global fraction of baryonic matter and dark matter. Moreover, it is necessary to assume that the baryonic fraction from clusters does not depend on the redshift [14]. This assumption is valid if one considers that these clusters are formed approximately by the same time.¹ (see [15] for more details). Thus, the gas mass fraction can be defined as, $f_{gas} \equiv M_{gas}/M_{tot}$, where M_{gas} is the X-rays gas mass and M_{tot} is the total gravitational mass of GC respectively. To relate f_{gas} with the parameters of a particular cosmological model we can write M_{gas} and M_{tot} in terms of $d_A(z)$ as follows [16],

$$f_{gas}^{\Lambda CDM}(z) \equiv \frac{b}{1 + \alpha} \frac{\Omega_b}{\Omega_{0m}} \left(\frac{d_A^{\Lambda CDM}(z)}{d_A(z)} \right)^{3/2}, \quad (5)$$

where $d_A(z)$ is the angular diameter distance for a given cosmological model and $d_A^{\Lambda CDM}(z)$ is the angular diameter distance for a reference model, in this case, let us assume the ΛCDM model. Here, Ω_b and Ω_{0m} are the baryonic density parameter and the dark matter density parameter, respectively. The parameter b is the depletion factor which relates the baryonic fraction in clusters to the mean cosmic value. The constant α is the ratio between optically luminous baryonic mass in galaxies (stellar mass) to the baryonic X-ray gas mass in intracluster medium, and its value is given by $\alpha \approx 0.19\sqrt{h}$ [15]. The factor h is the normalized Hubble constant, that is, $h = H_0/100 \text{ km.s}^{-1} \text{ Mpc}^{-1}$. Let us use the f_{gas} measurements from 42 GC obtained in [17]. The χ^2 is defined as

$$\chi_{f_{gas}}^2(z_i, \Theta) = \sum_{i=1}^{42} \frac{[f_{gas}^{\Lambda CDM}(z_i, \Theta) - f_{gas}(z_i, \Theta)]^2}{\sigma_{f_{gas}}^2} + \left(\frac{\Omega_b h^2 - 0.0214}{0.0020} \right)^2 + \left(\frac{h - 0.72}{0.08} \right)^2 + \left(\frac{b - 0.824}{0.089} \right)^2, \quad (6)$$

where f_{gas} is observational gas mass fraction data [17] and $\sigma_{f_{gas}}$ are the systematic errors. In the analysis, we have considered $b = 0.824$ [15].

C. Gravitational lensing

The gravitational lens effect is one of the queen's tests of General Relativity. Strong gravitational lensing occurs when the light rays of a source are strongly deflected by the lens producing multiples images. The position of these images depend on the properties of the lens mass distribution [18]. Because the Einstein radii, θ_E , also depends on a cosmological model, the SL observations can be used as an additional method to probe the nature of the DE [3, 19]. In this work, we use the method which consists in comparing the ratio \mathcal{D} of angular diameter distances between lens and source, $d_A(z_l, z_s)$, and between observer and lens, $d_A(0, z_s)$, with its observable counterpart \mathcal{D}^{obs} given by

$$\mathcal{D}(z_l, z_s) = \frac{d_A(z_l, z_s)}{d_A(0, z_s)} = \frac{\int_{z_l}^{z_s} dz'/E(z', \Theta)}{\int_0^{z_s} dz'/E(z', \Theta)}, \quad (7)$$

$$\mathcal{D}^{obs} = \frac{c^2 \theta_E}{4\pi \sigma_{SIS}^2}, \quad (8)$$

where σ_{SIS} is the Singular Isothermal Sphere (SIS) velocity dispersion and $E(z, \Theta) \equiv H(z, \Theta)/H_0$, being $H(z, \Theta)$ the Hubble function. In order to put constraints on cosmological parameters through $E(z, \Theta)$, the Einstein radius θ_E and the dispersion velocity σ_{SIS} (Exactly its central velocity dispersion σ_0) must be obtained by astrometric and spectroscopic means respectively. In the first case, it depends on the lens modelling (either SIS, Singular Isothermal Ellipsoid (SIE) or Navarro-Frenk-White density profiles). In the second case, the velocity dispersion σ_{SIS} of the mass distribution and the observed stellar velocity dispersion σ_0 need not be the same, since the halos of dark matter can

¹ Even though GC form at the same time, they can have different evolution and so different gas fraction. To preserve the constancy of the baryon fraction with redshift to mimic the relative cosmic abundance, GC have to be selected among the most massive and relaxed ones at each epoch.

have a greater speed of dispersion than the visible stars [20]. These effects can be taken into account through the following relationship $\sigma_{SIS} = f_E \sigma_0$, where the parameter f_E emulates the systematic errors in the rms due to the difference between σ_{SIS} and σ_0 ; the rms error caused by assuming the SIS model, since the observed image separation does not directly correspond to θ_E and softened SIS potentials which tend to decrease the typical image separations [21]. In the present work we assume the best-fit reported in [19] (and references therein), where $f_E \approx 1$, which has been properly marginalized. On the other hand, GC can also act as sources to produce strong gravitational lensing showing giant arcs around GC. This phenomenon can be used to constrain the astrophysical properties of the cluster (projected mass) and cosmology [22]. If we assume the condition of hydrostatic equilibrium ² and an approximation of spherical symmetry ³ [23], then a theoretical surface density can be described as

$$\Sigma_{th} = \frac{3}{2G\mu m_p} \frac{k_B T_X \beta_X}{d_A(0, z_l) \theta_c}, \quad (9)$$

where k_B , m_p , $\mu = 0.6$ and β_X are, respectively, the Boltzmann constant, the proton mass, the mean molecular weight and the slope of the β -model [24]. Although the hydrostatic equilibrium and isothermal hypotheses are very strong, the total mass density obtained under such assumption may lead to good estimates, even in dynamically active GC with irregular morphologies in X-Ray. Then, combining this with the critical surface mass density for lensing Σ_{obs} [25], We can get a Hubble constant independent ratio as

$$\mathcal{D}^{obs} = \frac{d_A(z_l, z_s)}{d_A(0, z_s)} = \frac{\mu m_p c^2}{6\pi} \frac{1}{k_B T_X \beta_X} \sqrt{\theta_t^2 + \theta_c^2}, \quad (10)$$

where the parameters T_X , β_X and θ_c can be obtained from X-Ray observational data. The position of tangential critical curve $\theta_t = \epsilon \theta_{arc}$, where θ_{arc} is the observational arc position and $\epsilon = (1/\sqrt{1.2}) \pm 0.04$ quantifies the slight difference with arc radius angle (See [26, 27] for more details about the priors and 10 galaxy clusters used as sample).

In the present work we use a sample of 80 strong lensing systems by [19], which contains 70 data points from SLACS and LSD and 10 data points from GC. Again, the fit of the theoretical models to strong lensing observations can be found by the minimization of

$$\chi_{SL}^2 = \sum_{i=1}^{80} \frac{(\mathcal{D}_i^{obs} - \mathcal{D}_i^{th})^2}{\sigma_{\mathcal{D},i}^2}, \quad (11)$$

where the sum is over the sample and $\sigma_{\mathcal{D},i}^2$ denotes the variance of \mathcal{D}_i^{obs} .

Additionally to these data sets defined in the subsection II A, II B, and II C, let us use 580 Supernovae data (SNIa) from Union 2.1 [28], the CMB shift parameter (Planck 2013) [29, 30], as well as data from BAO (BOSS, WiggleZ, SDSS, 6dFGS) observations, adopting the three measurements of $A(z)$ obtained from [31, 32], and using the covariance among these data given in [33]. Each χ^2 function is constructed in a way analogous to the other tests considered above (see Appendix B).

D. Statistic analysis

Maximum likelihood \mathcal{L}_{max} , is the procedure of finding the value of one or more parameters for a given statistic which makes the known likelihood distribution a maximum. The maximum likelihood estimate for the best fit parameters p_i^m is

$$\mathcal{L}_{max}(p_i^m) = \exp \left[-\frac{1}{2} \chi_{min}^2(p_i^m) \right]. \quad (12)$$

If $\mathcal{L}_{max}(p_i^m)$ has a Gaussian errors distribution, then $\chi_{min}^2(p_i^m) = -2 \ln \mathcal{L}_{max}(p_i^m)$, which is our case [34]. In order to find the best values of the free parameters of the model, let us consider

² The pressure gradient force of an isothermal gas with temperature T_X is balanced by the gravity in GC.

³ Specifically a hydrostatic isothermal spherical symmetric β -model.

$$\chi_{total}^2 = \chi_{SNIa}^2 + \chi_{CMB}^2 + \chi_{BAO}^2 + \chi_{d_A}^2 + \chi_{f_{gas}}^2 + \chi_{SGL}^2. \quad (13)$$

The Fisher matrix is widely used in the analysis of the constraint of cosmological parameters from different observational data sets [35, 36]. They encode the Gaussian uncertainties σ_i^2 of the several parameters p_i^m . Given the best fit $\chi_{min}^2(p_i^m, \sigma_i^2)$, the Fisher matrix can be calculated as

$$F_{ij} = \frac{1}{2} \frac{\partial^2 \chi_{min}^2}{\partial p_i^m \partial p_j^m}, \quad (14)$$

where $F_{ij} = F_{ij}(p_i^m, \sigma_i^2)$ also depends on the uncertainties σ_i^2 of the observables p_i^m for each model m . The inverse of the Fisher matrix provides an estimate of the covariance matrix through $[C_{cov}] = [F]^{-1}$. Its diagonal elements are the squares of the uncertainties in each parameter marginalizing over the others, while the off-diagonal terms yield the correlation coefficients between parameters. The uncertainties obtained in the propagation of errors are given by $\sigma_i = \sqrt{Diag[C_{cov}]_{ij}}$. Notice that the marginalized uncertainty is always greater than (or at most equal to) the non-marginalized one: marginalization can't decrease the error, and only has no effect if all other parameter are uncorrelated with it⁴. Previously known uncertainties on the parameters, known as priors, can be trivially added to the calculated Fisher matrix. This is manifestly the case for us: A lot of standard cosmological datasets provide priors on our previously defined cosmological parameters. The analysis with the Fisher matrix is used to evaluate the errors on the best-fit parameters.

In our results, let us consider different cosmological models. Thus, a way to quantify which model best fit the data is consider a Bayesian comparison. We adopted the Akaike and Bayesian information criterion (AIC and BIC, respectively), which allows us to compare cosmological models with different degrees of freedom, with respect to the observational evidence and the set of parameters [37]. The AIC and BIC can be calculated as

$$AIC = -2 \ln \mathcal{L}_{max} + 2d, \quad (15)$$

$$BIC = -2 \ln \mathcal{L}_{max} + d \ln N, \quad (16)$$

where \mathcal{L}_{max} is the maximum likelihood of the model under consideration ($\mathcal{L}_{max} = \exp[-\frac{1}{2}\chi_{min}^2]$), d is the number of parameters and N the number of data points. The BIC imposes a strict penalty against extra parameters for any set with N data. The preferred model is that which minimizes the AIC and BIC. However, the absolute values of them are not of interest, only the relative values between the different models [38]. Therefore the “strength of evidence” can be characterized in the form $\Delta AIC = AIC_i - AIC_{min}$, $\Delta BIC = BIC_i - BIC_{min}$, where the subindex i refers to value of AIC (BIC) for model i and AIC_{min} (BIC_{min}) is the minimum value of AIC (BIC) among all the models [39]. We give the judgements for both criterion as follows: (i) If $\Delta AIC(\Delta BIC) \leq 2$, then the concerned model has substantial support with respect to the reference model (i.e. it has evidence to be a good cosmological model), (ii) if $4 \leq \Delta AIC(\Delta BIC) \leq 7$ it is an indication for less support with respect to the reference model, and finally, (iii) if $\Delta AIC(\Delta BIC) \geq 10$ then the model has no observational support. Thus, if we have a set of models of dark energy first we should estimate the best fit χ^2 and then we can apply the AIC and BIC to identify which model is the preferred one by the observations. We also apply the reduced chi-square to see how well the model fit the data, Which is defined as $\chi_{red}^2 = \chi_{min}^2/\nu$, where ν is the degrees of freedom usually given by $N - d$. Table VI shows the values of d , χ_{red}^2 , AIC and BIC for the DE models from all cosmological tests, whose data points are: SNIa (580), CMB (3), BAO (7), d_A (25), f_{gas} (42), SGL (80). Priors used in the present analysis are standard and most conservative possible and combining GC data with independent constraints from CMB, BAO and SNIa removes the need of priors for Ω_b and h leads to tighter constraints over Ω_m , Ω_k and the parameters that characterize the dark energy density for different cosmological models. On the other hand, SGL offers a great opportunity to constrain dark energy features without prior assumptions on the fiducial cosmology.. In what follows we present our main results.

⁴ For an unbiased estimator, If all the parameters are assumed to be known (in other words, if we don't marginalize over any other parameters), then the minimal expected error is $\sigma_i = 1/\sqrt{F_{ij}}$.

III. DARK ENERGY MODELS AND RESULTS

In order to put constraints on DE cosmological models using GC (d_A , f_{gas}) and SGL, we need to calculate the theoretical angular diameter distance of the model and then compare it with the observations. In addition, to investigate whether a cosmological model can predict an accelerated expansion phase of the Universe, we must study the behavior of the deceleration parameter $q(z)$. The angular diameter distance for a Friedmann-Lemaître-Robertson-Walker model universe, for a source at redshift z is

$$d_A(z, \Theta) = \frac{3000h^{-1}}{(1+z)} \frac{1}{\sqrt{|\Omega_k|}} \sin \varsigma \left(\int_0^z \frac{\sqrt{|\Omega_k|}}{E(z, \Theta)} dz \right), \quad (17)$$

where $h = H_0/100 \text{ km.s}^{-1} \text{ Mpc}^{-1}$ is dimensionless Hubble parameter and the function $\sin \varsigma(x)$ is defined such that it can be $\sinh(x)$ when $\Omega_k > 0$, $\sin(x)$ when $\Omega_k < 0$ and x when $\Omega_k = 0$ [40]. In the standar FLRW cosmology, the expansion rate as a function of the scale factor $H(a)$ is given by the Friedmann equation as

$$E^2(a, \Omega_i) = \Omega_r a^{-4} + \Omega_m a^{-3} + \Omega_k a^{-2} + \Omega_X e^{3 \int_a^1 \frac{da'}{a'} (1+w(a'))}, \quad (18)$$

where $H(a)/H_0 = E(a, \Omega_i)$, H_0 is the curret value of the expansion rate and the scale factor is related to redshift as $1+z = a^{-1}$, such that $a_0 = 1$ at present. In the equation (18) Ω_i is the current energy density divided by the critical density today $\rho_{cri} = 3H_0^2/8\pi G$. In the form of the i -th component of the fluid density of: radiation (Ω_r), matter (Ω_m), curvature (Ω_k) and dark energy (Ω_X). $\Omega_{r0}(h) = \Omega_\gamma(h)(1 + 0.2271N_{eff})$, where $\Omega_\gamma(h) = 2.46910^{-5}h^{-2}$ is the density of photons and $N_{eff} = 3.046$ is the effective number of neutrino species [41]. The ratio of the pressure to the energy density $\omega(a) = p(a)/\rho(a)$ is the EoS of dark energy, which divide our models into two cases: when the energy density of the fluid is constant and the other the energy density of the fluid is dynamic. In all cosmological models, the density parameter of curvature Ω_k is left free to vary and constraints on it are obtained. A vector of parameters is considered for each model of dark energy $\Theta_i^{model} = \{\theta_i, \Omega_i\}$, where $\theta_i = \{h, \Omega_b\}$ for the analysis of the present work.

A. Λ CDM

We begin our analysis with the standard cosmological model. In this paradigm, the DE is provided by the cosmological constant Λ . The expansion rate within Λ CDM context is determined by

$$E^2(z, \Theta) = \Omega_r(1+z)^4 + \Omega_m(1+z)^3 + \Omega_k(1+z)^2 + \Omega_\Lambda, \quad (19)$$

where Ω_r , Ω_m and $\Omega_\Lambda = 1 - \Omega_m - \Omega_k - \Omega_r$, are the density parameters for radiation, matter and DE, respectively. Here, the free parameter vector is $\Theta_i = \{h, \Omega_b, \Omega_m, \Omega_k\}$. We find the best fit of parameters at 1σ confidence level (CL) (and hereafter), whose results are shown in Table I.

Parameter	CMB+BAO+SNIa	CMB+BAO+SNIa+ d_A + f_{gas} +SGL
h	0.6858 ± 0.0095	0.7063 ± 0.0067
Ω_m	0.2981 ± 0.0093	0.2839 ± 0.0046
Ω_k	-0.0011 ± 0.0031	0.0048 ± 0.0024
Ω_b	0.0475 ± 0.0014	0.04411 ± 0.00099
χ_{min}^2	565.686	777.256

TABLE I: Summary of the best fit values for Λ CDM model.

In Table I we can see the impact of adding the GC and SGL tests to the more traditional ones (CMB+BAO+SNIa), which evidently improves the constraints on the parameters of the model (and hereafter for each model).

B. w CDM model

The most simple extension of the Λ CDM model is to consider that the equation of state (EoS) still is constant but its value can deviate of -1 . In this case, the expansion rate $E^2(z, \Theta)$ for a FLRW universe with curvature reads as

$$E^2(z, \Theta) = \Omega_r(1+z)^4 + \Omega_m(1+z)^3 + \Omega_k(1+z)^2 + \Omega_X(1+z)^{3(1+w)}, \quad (20)$$

where $\Omega_X = (1 - \Omega_m - \Omega_k - \Omega_r)$. In this model, the set of free parameters is $\Theta = \{h, \Omega_b, \Omega_k, \Omega_m, \omega\}$. As in the case of Λ CDM model, first we estimate the best fit values using the data from *SNIa + CMB + BAO* alone. Then, we use the full data set, that is, *SNIa + CMB + BAO + d_A + f_{gas} + SGL*. The best fit values at 1σ CL for this case is shown in the Table II.

Parameter	<i>CMB+BAO+SNIa</i>	<i>CMB+BAO+SNIa+d_A+f_{gas}+SGL</i>
h	0.6897 ± 0.0098	0.7080 ± 0.0070
Ω_m	0.2964 ± 0.0093	0.2839 ± 0.0049
Ω_k	-0.0028 ± 0.0033	0.0007 ± 0.0028
ω	-1.057 ± 0.041	-1.086 ± 0.038
Ω_b	0.0468 ± 0.0014	0.0437 ± 0.0010
χ^2_{min}	563.953	772.283

TABLE II: Summary of the best fit values for wCDM model

Notice that in both cases the EoS has a phantom behavior and the standard model is excluded at least to 2σ CL (see Fig 1). As the case of Λ CDM model, the curvature parameter changes from negative to positive (Table II).

C. Chevalier-Polarski-Linder model

Another simple extension to the Λ CDM model is to allow that the EoS of the DE varies with the redshift. Several parameterizations have been considered in the literature. Here, let us consider the popular Chevallier-Polarski-Linder (CPL) model [42] [43]

$$w(z) = w_0 + w_1 \frac{z}{1+z}, \quad (21)$$

where w_0 and w_1 are constants to be fitted. The parameter w_1 evaluates the dynamic character of the DE. The dimensionless Hubble expansion $E(z)$ for CPL is given by

$$E^2(z) = \Omega_r(1+z)^4 + \Omega_k(1+z)^2 + \Omega_m(1+z)^3 + \Omega_X X(z), \quad (22)$$

where $\Omega_X = (1 - \Omega_k - \Omega_m - \Omega_r)$ and

$$X(z) = (1+z)^{3(1+w_0+w_1)} \exp \left[-\frac{3w_1 z}{1+z} \right]. \quad (23)$$

The free parameters to be constrained here are $\Theta = \{h, \Omega_b, \Omega_k, \Omega_m, w_0, w_1\}$. The best fit values at 1σ CL using *CMB + BAO + SNIa* and all the cosmological tests (full analysis) are summarized in Table III.

For this case we can see that the EoS at present has a quintessential behavior and the curvature parameter Ω_k remains negative.

D. Interacting Dark Energy model

Cosmological models where dark matter and DE are non minimally coupled throughout the evolution history of the Universe, have been considered to solve/assuage the problem of the cosmic coincidence as well as the problem of the cosmological constant (models where dark matter interacts with vacuum energy). See [44, 45] for general review. It has recently been shown that the current observational data can favor the late-time interaction in the dark sector [46–51]. In general, we assume that dark matter and DE interact via a given coupling function Q given by

<i>Parameter</i>	<i>CMB+BAO+SNIa</i>	<i>CMB+BAO+SNIa+d_A+f_{gass}+SGL</i>
h	0.686 ± 0.011	0.7059 ± 0.0075
Ω_m	0.299 ± 0.010	0.2865 ± 0.0058
Ω_k	-0.0075 ± 0.0044	-0.0032 ± 0.0035
ω_0	-0.88 ± 0.17	-0.92 ± 0.15
ω_1	-1.05 ± 1.06	-1.09 ± 0.90
Ω_b	0.0472 ± 0.0015	0.0439 ± 0.0011
χ^2_{min}	564.428	807.075

TABLE III: Summary of the best fit values for CPL model

$$\begin{aligned}\dot{\rho}_m + 3H\rho_m &= Q\rho_m \\ \dot{\rho}_x + 3H(1+w_x)\rho_x &= -Q\rho_m,\end{aligned}\tag{24}$$

where ρ_m and ρ_x are the matter density and the dark energy density respectively with w_x the equation of state. Here $Q = \delta H$ characterizes the strength of the interacting through the dimensionless coupling term δ , which establishes a transfer of energy from dark energy to dark matter for $\delta > 0$, whereas for $\delta < 0$ the energy transfer is opposite. This model was originally introduced in [52], then investigated in various contexts [53–55]. The expansion rate of the Universe for this model is given by

$$\begin{aligned}E^2(z, \Theta) &= \Omega_r(1+z)^4 + \Omega_k(1+z)^2 + \Omega_m\Psi(z) \\ &\quad + \Omega_X(1+z)^{3(1+w_x)},\end{aligned}\tag{25}$$

where $\Omega_X = (1 - \Omega_m - \Omega_k - \Omega_r)$ and

$$\Psi(z) = \frac{(\delta(1+z)^{3(1+w_x)} + 3w_x(1+z)^{3-\delta})}{\delta + 3w_x}\tag{26}$$

This model is characterized by six parameters $\Theta = \{h, \Omega_b, \Omega_k, \Omega_m, w_x, \delta\}$. We show the best fit values of these parameters in Table IV.

<i>Parameter</i>	<i>CMB+BAO+SNIa</i>	<i>CMB+BAO+SNIa+d_A+f_{gass}+SGL</i>
h	0.698 ± 0.011	0.7186 ± 0.0097
Ω_m	0.3326 ± 0.0098	0.3201 ± 0.0049
Ω_k	0.0038 ± 0.0096	0.0211 ± 0.0044
ω_x	-1.018 ± 0.053	$-0.816^{+0.026}_{-0.14}$
δ	-0.0103 ± 0.0066	$-0.0188^{+0.026}_{-0.0011}$
Ω_b	0.0442 ± 0.0048	0.0424 ± 0.0012
χ^2_{min}	563.256	806.794

TABLE IV: Summary of the best fit values from for IDE model.

It is interesting to appreciate for this model the change in the EoS at present from a phantom behavior to one of quintessence and the curvature parameter Ω_k is positive for both cases. We can also notice that the case $\delta = 0$ (absence of interaction) is excluded at least to 2σ CL for the present analysis, where we can appreciate that for both data sets the transfer of energy is from dark matter to dark energy (see Fig 1).

E. Early Dark Energy model

In the early dark energy (EDE) scenarios it is proposed that the energy density of DE can be significant at high redshifts. This can be if the DE tracks the dynamics of the background fluid density [56]. Here, we generalize the EDE model proposed by [57] adding a curvature term. The dimensionless Hubble function for this model is

$$E^2(z, \Theta) = \frac{\Omega_r(1+z)^4 + \Omega_m(1+z)^3 + \Omega_k(1+z)^2}{1 - \Omega_X}, \quad (27)$$

where Ω_X is given by

$$\Omega_X = \frac{\Omega_{X_0} - \Omega_e [1 - (1+z)^{3w_0}]}{\Omega_{X_0} + f(z)} + \Omega_e [1 - (1+z)^{3w_0}] \quad (28)$$

and

$$f(z) = \Omega_m(1+z)^{-3w_0} + \Omega_r(1+z)^{-3w_0+1} + \Omega_k(1+z)^{-3w_0-1}, \quad (29)$$

such that $\Omega_{X_0} = 1 - \Omega_m - \Omega_k - \Omega_r$ is the current DE density, Ω_e is the asymptotic early dark energy density and w_0 is the present dark energy equation of state. Here, we have six free parameters $\Theta = \{h, \Omega_b, \Omega_k, \Omega_m, \Omega_e, \omega_0\}$. The best fit values of the model parameters are summarized in Table V.

<i>Parameter</i>	<i>CMB+BAO+SNIa</i>	<i>CMB+BAO+SNIa+d_A+f_{gass}+SGL</i>
<i>h</i>	0.727 ± 0.019	0.714 ± 0.011
<i>Ω_m</i>	0.295 ± 0.011	0.3241 ± 0.0053
<i>Ω_k</i>	0.0083 ± 0.0067	0.0138 ± 0.0041
<i>Ω_e</i>	0.047 ± 0.028	0.055 ± 0.015
<i>ω₀</i>	-1.119 ± 0.061	-1.151 ± 0.054
<i>Ω_b</i>	0.0421 ± 0.0023	0.0421 ± 0.0012
<i>χ_{min}²</i>	564.321	803.996

TABLE V: Summary of the best fit values for EDE model.

For this model the EoS maintains a phantom behavior at the present time and Ω_k is positive in both cases.

Fig 1 shows two-dimensional parametric spaces at 1σ and 2σ CL for the some models discussed here from a joint analysis, namely *SNIa + CMB + BAO + d_A + f_{gass} + SGL*, where we can appreciate complementary information to the main results obtained that characterize the different cosmological models of dark energy studied in the present work.

F. Statistical discrimination models

In Table VI we present the values for the analysis of the information criterion with respect to the five cosmological models presented above, for used data set, namely *CMB+BAO+SNIa+d_A+f_{gass}+SGL*. As we can see, ΔAIC and ΔBIC for Λ CDM and ω CDM are approximately equal or less than five and hence these models are very efficient and in very good agreement with observations, while for the other models this value is greater than ten, and therefore, according to this criterion CPL, IDE and EDE are not so favored by observational data.

IV. HISTORY OF THE EXPANSION AND COSMOGRAPHY

Is natural to describe the kinematics of the cosmic expansion through the Hubble parameter $H(t)$ and its dependence on time, i.e. the deceleration parameter $q(t)$ [58]. Following [59], the scale factor $a(t)$ expands into a Taylor series around the current time (t_0) as:

$$\frac{a(t)}{a(t_0)} = 1 + \frac{H_0}{1!} [t - t_0] - \frac{q_0}{2!} H_0^2 [t - t_0]^2 + \frac{\dot{q}_0}{3!} H_0^3 [t - t_0]^3 + \dots, \quad (30)$$

where in general we can have a kinematic description of the cosmic expansion through the set of parameters:

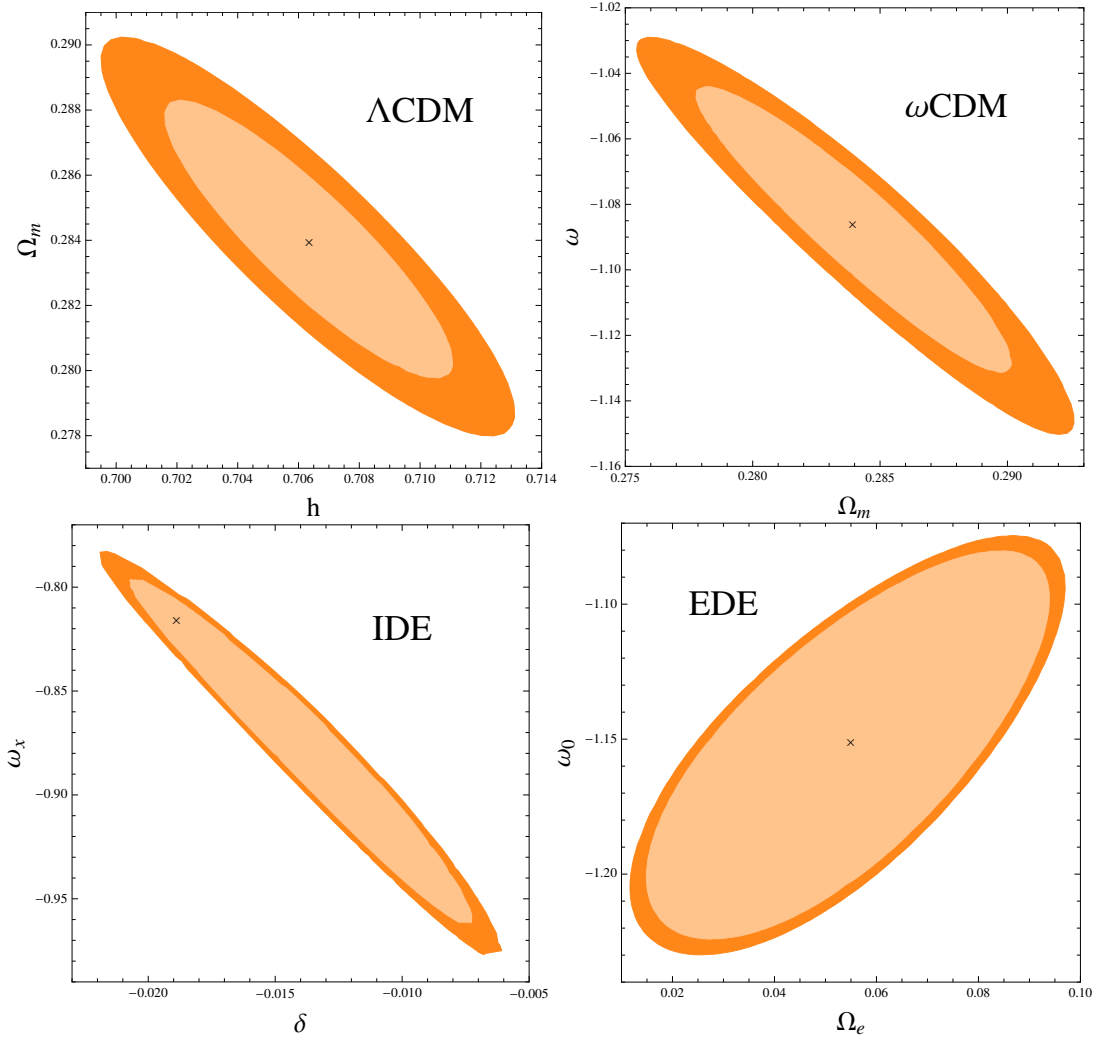


FIG. 1: 1σ and 2σ two-dimensional confidence contours parameters of some cosmological models discussed here, where the main results of the analysis are shown using the combined data sets (CMB+BAO+SN Ia+ d_A + f_{gass} +SGL).

Model	d	χ^2_{red}	AIC	BIC	ΔAIC	ΔBIC
ΛCDM	4	1.06	783.859	803.666	4.972	0.000
ωCDM	5	1.05	778.886	805.296	0.000	1.629
CPL	6	1.10	813.678	846.691	34.791	43.024
IDE	6	1.10	813.397	846.410	34.510	42.743
EDE	6	1.09	810.599	843.612	31.712	39.945

TABLE VI: AIC and BIC analyses for different dark energy models using the combined analysis data sets (CMB+BAO+SN Ia+ d_A + f_{gass} +SGL), where $N=737$ and $\chi^2_{red} = \chi^2_{min}/\nu$.

$$H(t) \equiv \frac{1}{a} \frac{da}{dt}; q(t) \equiv -\frac{1}{a} \frac{d^2a}{dt^2} H(t)^{-2}; j(t) \equiv \frac{1}{a} \frac{d^3a}{dt^3} H(t)^{-3}, \quad (31)$$

where the last term is known as jerk parameter $j(t)$. The great advantage of this method is that we can investigate the cosmic acceleration without assuming any modification of gravity theory or dark energy model, due mainly to its geometric approximation. Although more terms of the series can be analyzed, we are only interested in the first three terms for the present work. The deceleration and jerk parameter are obtained as

$$q(z) = -1 + \frac{(1+z)}{H(z)} \frac{dH(z)}{dz} \quad (32)$$

and

$$j(z) = q^2 + \frac{(1+z)^2}{H(z)} \frac{d^2H(z)}{dz^2}. \quad (33)$$

To characterize whether the universe is currently accelerated or decelerated, the history of expansion is fit through deceleration parameter $q(z) \equiv -\ddot{a}(z)/a(z)H(z)^2$. If $q(z) > 0$, $\ddot{a}(z) < 0$; then the expansion decelerate, as expected due to gravity (i.e. dark matter, baryonic matter, radiation). The discovery that the universe is currently accelerating, already has about one decade and a half old [60] [61]. The simplest explanation for the accelerating universe is the cosmological constant Λ , however, there is still no compelling theoretical explanation based on physical foreground and not only phenomenological. To take into account information about the dynamics of the expansion we use (18) and (31), then we obtain (32) and (33), which directly depends on the cosmological model and its matter-energy content. In general, if $\Omega_X \neq 0$ is sufficiently large (i.e. $\Omega_X > \Omega_m$), then $q(z) < 0$ and $\ddot{a}(z) > 0$, which corresponds to an expansion accelerated the universe as shown by observational data at present, which also indicates a cosmological constant different from zero. If the acceleration of the universe is driven by a new fluid, then it is important to identify signs to determine if the energy density of the fluid is constant or dynamic.

Model	χ_{red}^2	Parameters
Λ CDM	1.09	$h = 0.72 \pm 0.12$, $\Omega_m = 0.268 \pm 0.008$, $\Omega_k = -0.13 \pm 0.16$.
ω CDM	1.11	$h = 0.72 \pm 0.12$, $\Omega_m = 0.268 \pm 0.009$, $\Omega_k = -0.17 \pm 0.88$, $\omega = -0.973 \pm 0.682$.
CPL	1.17	$h = 0.70 \pm 0.14$, $\Omega_m = 0.286 \pm 0.012$, $\Omega_k = -0.98 \pm 2.21$, $\omega_a = -1.50 \pm 2.33$, $\omega_0 = -0.45 \pm 0.17$
IDE	1.18	$h = 0.72 \pm 0.10$, $\Omega_m = 0.273 \pm 0.011$, $\Omega_k = -0.11 \pm 1.58$, $\omega_x = -0.95^{+0.79}_{-0.29}$, $\delta = 4.08^{+13.80}_{-6.51}$
EDE	1.18	$h = 0.72 \pm 0.11$, $\Omega_m = 0.276 \pm 0.014$, $\Omega_k = -0.43 \pm 1.68$, $\omega_0 = -0.98^{+0.27}_{-4.51}$, $\Omega_e = -0.93^{+1.08}_{-3.08}$

TABLE VII: The best fit values for the free parameters using data from GC ($d_A + f_{gas}$). We use the mean value $\Omega_b h^2$ from [29] and $\chi_{red}^2 = \chi_{min}^2/\nu$.

In the present cosmographic analysis we made use of data from GC ($d_A + f_{gas}$), where we can see that these does not provide a tight constraints on curvature and dark energy parameters, mainly due to the degeneracy presented between these parameters and the large systematic errors of the samples (See Table VII), which can lead to large discrepancies with respect to the standard model. Despite this, we are more interested in the analysis of the behavior of low redshift of each cosmological model with respect to these data set. Figure 2 shows the plot of the deceleration parameter $q(z)$ using data only from GC. As expected, the models studied give $q(z) < 0$ at late times and $q(z) > 0$ at earlier epoch, which means that the history of the expansion is slowed down in the past and speeded up at present. All cosmological models presents a redshift of transition (z_t) between the two periods (see Figure 2), however, all models of dynamical dark energy present an interesting behavior of slowing down of acceleration at low redshift (late times) using only data from BAO, which can be characterized through the change of sign of the parameter $j(z)$ (CPL: $j(z_{low}) \rightarrow 0$, when $z_{low} \sim 0.42$; IDE: $j(z_{low}) \rightarrow 0$, when $z_{low} \sim 0.83$; EDE: $j(z_{low}) \rightarrow 0$, when $z_{low} \sim 0.16$). We can interpret $j(z)$ as the slope at each point of $q(z)$, which indicates a change in acceleration. This result is consistent with the one presented by J. Barrow, R. Bean and J. Magueijo [62], who raises the possibility of a scenario consistent with the current accelerating universe and does not involve an eternal accelerated expansion. In [59] an extensive analysis of this possibility is made. This can be also a clear behavior of dynamical dark energy at low redshift for these models with variation of the density of dark energy over time.

V. SUMMARY AND DISCUSSION

In the present work we compared alternative cosmological models of dark energy using data obtained from GC and SGL in addition to more traditional ones, getting the best-fit value of parameters for each one. **On the other hand**, applying the Akaike an Bayesian information criteria we determine which of these models is the most favored by current observational data. Our analysis shows that ω CDM and Λ CDM dark energy models are preferred by

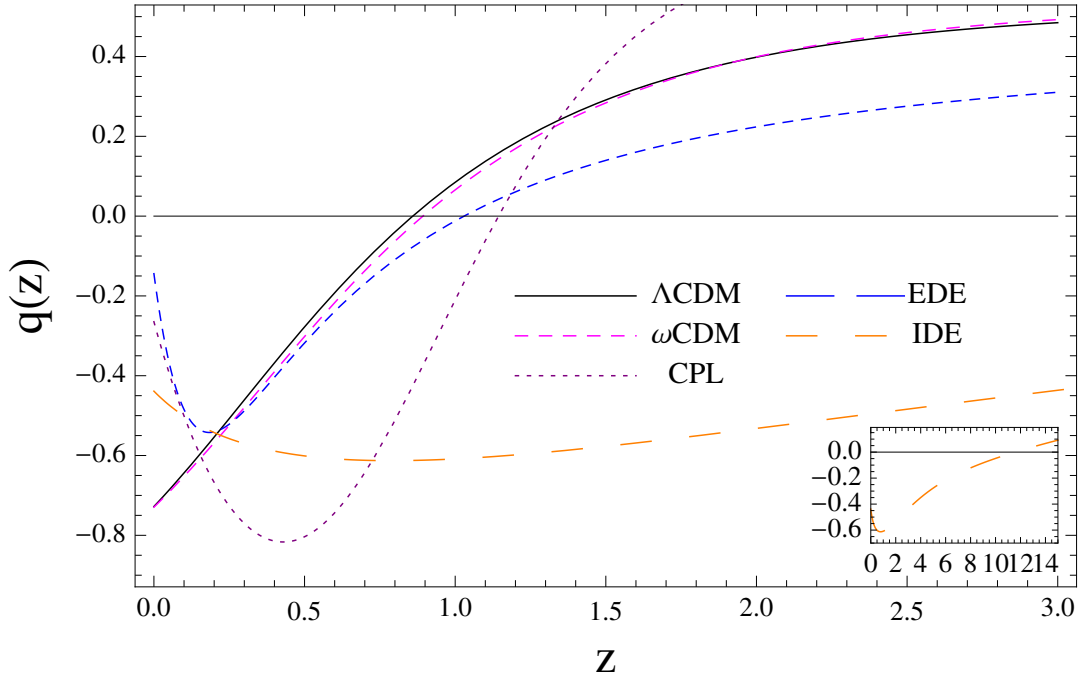


FIG. 2: Deceleration parameter vs redshift using only GC data ($d_A + f_{gas}$). It is shown the transition decelerated-accelerated ($q(z_t) = 0$) and the current value of (q_0) (Λ CDM ($z_t \sim 0.85$, $q_0 = -0.72$), ω CDM ($z_t \sim 0.88$, $q_0 = -0.72$), CPL ($z_t \sim 1.13$, $q_0 = -0.27$), IDE ($z_t \sim 11.43$, $q_0 = -0.44$), EDE ($z_t \sim 1.1$, $q_0 = -0.15$)). Notice the strange behavior of the deceleration parameter to later times for models of dynamical dark energy (CPL, IDE, EDE).

AIC and BIC. For the first time we report that the ω CDM model is favored by observational data at least with AIC, however, the Λ CDM model remains the best fit for BIC (See Table VI). In Figure 1 we can see that Λ CDM model is excluded at least 2σ CL for ω CDM, IDE and EDE models, combining all data set (see too Tables II, IV and V). Models as CPL, IDE and EDE are heavily penalized given their large number of free parameters.

On the other hand, we carry out the study of the history of cosmic expansion through the $H(z)$, $q(z)$ and $j(z)$ parameters with data from GC ($d_{A,clusters} + f_{gas}$). We find new evidence showing anomalous behavior of the deceleration parameter $q(z)$ in later times ($z_{low} < 0.5$), suggesting that the expansion of the universe could decelerate in the near future (Figure 2), which was pointed out in previous works with SNIa (for CPL [63, 64]), f_{gas} (for CPL and different parameterizations of $w(z)$ [65, 66]) and BAO (for CPL, IDE and EDE [67]). Under this perspective raises the possibility that an accelerated expansion does not imply the eternal expansion, even in the presence of dark energy [59]. This cosmic slowing down of acceleration only appears in dynamic models of dark energy (CPL, IDE and EDE), which in principle can be an indication of the need for a scalar field such as quintessence or phantom. Finally in Figure 3 we show the results for jerk parameter $j(z)$ obtained from our kinematic analysis, where we can appreciate a considerable deviation from Λ CDM (black curve) in late times ($z < 0.5$) for CPL, IDE and EDE models. A more careful study might give insight into this anomalous behavior, which may also represent a challenge for alternative models to dark energy including modified gravity models.

As we can see, the fit of observational data acquires slightly larger values of χ^2_{min} with respect to Λ CDM, when GC and SGL data are added to the more traditional ones as CMB+BAO+SNIa, which may be mainly due to their large systematic errors (GC+SGL) (See Tables I - V). However, the potential of these data sets as cosmological tests is very high since, for example, that increasing the number of data points and the reduction of systematic errors leads to better constraints in parameters such as energy dark, which is fundamental interest for the cosmology.

Acknowledgments

A. Bonilla and J. E. Castillo wish to acknowledge to the Universidad Distrital F.J.C. and FIZMAKO group for his academic support. A. Bonilla also wish to thank the Departamento de Física of the UFJF for his academic support

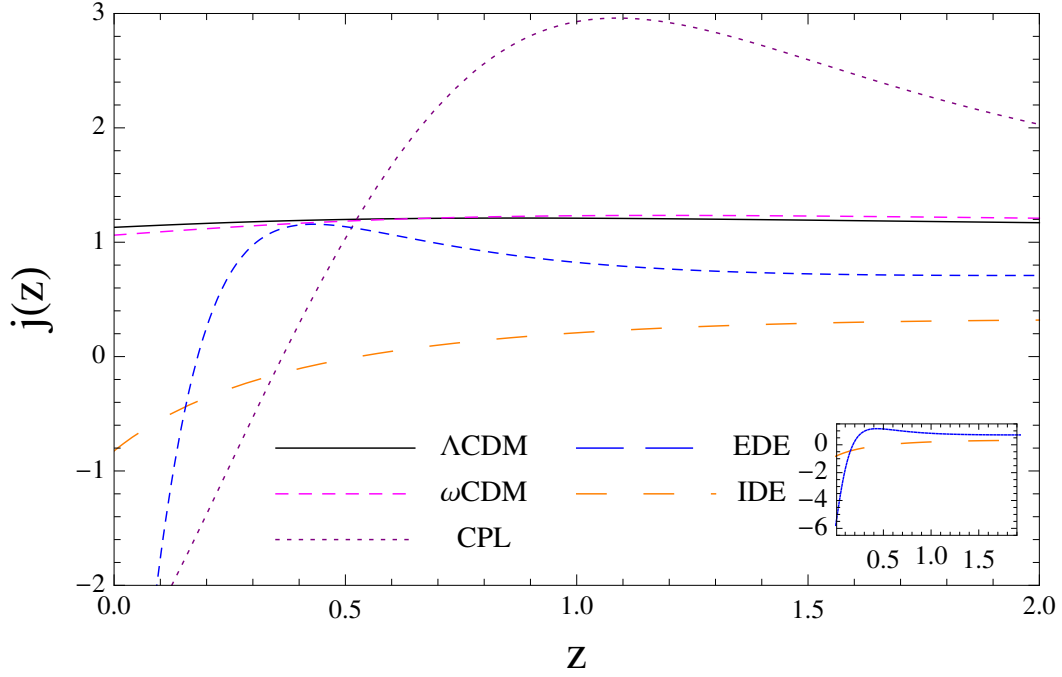


FIG. 3: Jerk parameter vs redshift using only GC data ($d_A + f_{gas}$). For cosmological models CPL, IDE and EDE, we can observe a strong deviation from Λ CDM to the present, while for w CDM this does not happen.

and to Rafael Nunes for constructive and fruitful discussions.

-
- [1] De Filippis, E., Sereno, M., Bautz, M. W. and Longo, G., *Measuring the Three-dimensional Structure of Galaxy Clusters. I. Application to a Sample of 25 Clusters*, 2005, *ApJ* 625, 108, [astro-ph/0502153].
 - [2] Bonamente, M., Joy, M. K., LaRoque, S.J., Carlstrom, J. E., Reese, E. D. & Dawson, K.S., *Determination of the Cosmic Distance Scale from Sunyaev-Zel'dovich Effect and Chandra X-Ray Measurements of High-redshift Galaxy Clusters*, 2006, *Astrophys. J.* 647 25 [astro-ph/0512349].
 - [3] Biesiada, M.; Piórkowska, A.; Malec, B., *Cosmic equation of state from strong gravitational lensing systems*, 2010, *MNRAS*, 406, 1055, [arXiv:1105.0946].
 - [4] Campigotto, M. C., Diaferio, A., Hernandez, X., & Fatibene, L. 2016, arXiv:1612.01535
 - [5] Albrecht, A., Bernstein, G., Cahn, R., et al. 2006, arXiv:astro-ph/0609591
 - [6] Frieman, J. A., Turner, M. S., & Huterer, D. 2008, *ARA&A*, 46, 385
 - [7] Copeland, E. J., Sami, M., & Tsujikawa, S., *Dynamics of dark energy*, 2006, *IJMP D* **15**, 1753, [arXiv:hep-th/0603057].
 - [8] Weinberg, S., *The cosmological constant problem*, 1989, *RMP* 61, 1.
 - [9] Bartelmann, M.; Steinmetz, M.; Weiss, A., *Arc statistics with realistic cluster potentials. 2: Influence of cluster asymmetry and substructure*, 1995, *A&A*, 297, 1, [astro-ph/9408082].
 - [10] Sunyaev RA, Zel'dovich YB., *The Spectrum of Primordial Radiation, its Distortions and their Significance*, 1970, *CoASP*, 2:66–74.
 - [11] Sunyaev, R. A. and Zel'dovich, Ia. B., *Microwave background radiation as a probe of the contemporary structure and history of the universe*, 1980, *ARAA*, 18, 537.
 - [12] Itoh, N., Kohyama, Y., & Nozawa, S. 1998, *ApJ*, 502, 7. [arXiv:astro-ph/9712289].
 - [13] Vikhlinin, A., Kravtsov, A. V., Burenin, R. A., et al. 2009, *ApJ*, 692, 1060. [arXiv:0812.2720].
 - [14] S. Sasaki, *A New method to estimate cosmological parameters using baryon fraction of clusters of galaxies*, Submitted to: *Publ.Astron.Soc.Jap.* [astro-ph/9611033].
 - [15] S. W. Allen, R. W. Schmidt, H. Ebeling, A. C. Fabian and L. van Speybroeck, *Constraints on dark energy from Chandra observations of the largest relaxed galaxy clusters*, 2004, *MNRAS* **353**, 457, [astro-ph/0405340].
 - [16] S. Nesseris and L. Perivolaropoulos, *Crossing the Phantom Divide: Theoretical Implications and Observational Status*, 2007, *JCAP* **0701**, 018, [astro-ph/0610092].
 - [17] S. W. Allen, D. A. Rapetti, R. W. Schmidt, H. Ebeling, G. Morris and A. C. Fabian, *Improved constraints on dark energy from Chandra X-ray observations of the largest relaxed galaxy clusters*, 2007, *MNRAS* **383**, 879 (2008), [arXiv:0706.0033]

- [astro-ph]].
- [18] Limousin, M.; Morandi, A.; Sereno, M.; Meneghetti, M.; Ettori, S.; Bartelmann, M.; Verdugo, T., *The Three-Dimensional Shapes of Galaxy Clusters*, 2012, [arXiv:1210.3067].
 - [19] Cao, S.; Pan, Y.; Biesiada, M.; Godlowski, W.; Zhu, Z-H, *Constraints on cosmological models from strong gravitational lensing systems*, 2012, JCAP, 03, 016, [arXiv:1105.6226].
 - [20] White, R. E., III, & Davis, D. S. 1996, Bulletin of the American Astronomical Society, 28, 41.04
 - [21] Narayan, R., & Bartelmann, M. 1996, In: Lectures on Gravitational Lensing, arXiv:astro-ph/9606001
 - [22] Sereno, M., & Longo, G. 2004, Mon. Non. Roy. Astron. Soc., 354, 1255
 - [23] Cavaliere, A., & Fusco-Femiano, R., "X-rays from hot plasma in clusters of galaxies", 1976, A&A, 49, 137
 - [24] Rosati, P., Borgani, S., & Norman, C., "The Evolution of X-ray Clusters of Galaxies", 2002, ARA&A, 40, 539
 - [25] Schneider, P., Ehlers, J., & Falco, E. E. 1992, Gravitational Lenses, XIV, 560 pp. 112 figs.. Springer-Verlag Berlin Heidelberg New York. Also Astronomy and Astrophysics Library, 112
 - [26] Ono, T., Masai, K., & Sasaki, S. 1999, PASJ, 51, 91
 - [27] Yu, H., & Zhu, Z.-H. 2011, Research in Astronomy and Astrophysics, 11, 776
 - [28] Suzuki, N., Rubin, D., Lidman, C., et al. 2012, ApJ, 746, 85
 - [29] Ade, P.A.R. *et al.*, *Planck 2013 results. XVI. Cosmological parameters*, 2013, [arXiv:1303.5076].
 - [30] Wang, Y., & Wang, S. 2013, Phys. Rev. D., 88, 043522
 - [31] Anderson L., Aubourg, E., Bailey, S., et al. 2012, Mon. Non. Roy. Astron. Soc., 427, 3435
 - [32] Blake, C., Kazin, E. A., Beutler, F., et al. 2011, Mon. Non. Roy. Astron. Soc., 418, 1707
 - [33] Shi K., Huang Y. & Lu T., *A comprehensive comparison of cosmological models from latest observational data*, 2012, MNRAS, **426**, 2452, [arXiv:1207.5875].
 - [34] Andrae, R., Schulze-Hartung, T., & Melchior, P. 2010, arXiv:1012.3754
 - [35] Albrecht A., Amendola L., Bernstein G., Clowe D., Eisenstein D., Guzzo L., Hirata C. and Huterer D. *et al.*, *Findings of the Joint Dark Energy Mission Figure of Merit Science Working Group*, 2009, [arXiv:0901.0721].
 - [36] Wolz, L., Kilbinger, M., Weller, J., & Giannantonio, T. 2012, J. Cosmology Astropart. Phys., 9, 009
 - [37] Schwarz, G., *Estimating the Dimension of a Model*, 1978, *The Annals of Statistics*, 6, 471.
 - [38] Liddle A. R., *How many cosmological parameters?*, 2004, MNRAS 351, L49-L53, [astro-ph/0401198v3].
 - [39] Burnham K. P. & Anderson D. R. 2003, *Model Selection and Multimodel Inference*, *Technometrics*, 45, 181.
 - [40] Hogg DW., *Distance measures in cosmology*, 1999, [astro-ph/9905116].
 - [41] Planck Collaboration, Ade, P. A. R., Aghanim, N., et al. 2014, A&A, 571, A16
 - [42] Chevallier M and Polarski D, *Accelerating Universes with Scaling Dark Matter*, 2001, *Int. J. Mod. Phys. D* 10, 213, [gr-qc/0009008].
 - [43] Linder E. V., *Mapping the Dark Energy Equation of State*, 2003, *Phys. Rev. Lett.*, 90, 091301, [astro-ph/0311403].
 - [44] Wang, B., Abdalla, E., Atrio-Barandela, F., & Pavón, D. 2016, Reports on Progress in Physics, 79, 096901
 - [45] Bolotin, Y. L., Kostenko, A., Lemets, O. A., & Yerokhin, D. A. 2015, International Journal of Modern Physics D, 24, 1530007
 - [46] Kumar, S., & Nunes, R. C. 2016, Phys. Rev. D., 94, 123511
 - [47] Kumar, S., & Nunes, R. C. 2017, arXiv:1702.02143
 - [48] Nunes, R. C., Pan, S., & Saridakis, E. N. 2016, Phys. Rev. D., 94, 023508
 - [49] Richarte, M. G., & Xu, L. 2015, arXiv:1506.02518
 - [50] Sharov, G. S., Bhattacharya, S., Pan, S., Nunes, R. C., & Chakraborty, S. 2017, Mon. Non. Roy. Astron. Soc., 466, 3497
 - [51] Salvatelli, V., Said, N., Bruni, M., Melchiorri, A., & Wands, D. 2014, Physical Review Letters, 113, 181301
 - [52] Wang, P., & Meng, X.-H. 2005, Classical and Quantum Gravity, 22, 283
 - [53] Costa, F. E. M., Barboza, E. M., Jr., & Alcaniz, J. S. 2009, Phys. Rev. D., 79, 127302
 - [54] Nunes, R. C., & Barboza, E. M. 2014, General Relativity and Gravitation, 46, 1820
 - [55] Yang, W., Banerjee, N., & Pan, S. 2017, arXiv:1705.09278
 - [56] Steinhardt P. J., Wang L., Zlatev I., *Cosmological tracking solutions*, 1999, Phys. Rev. D., 59, 123504, [astro-ph/9812313].
 - [57] Doran & Robbers, *Early Dark Energy Cosmologies*, 2006, J. Cosmology Astropart. Phys., 6, 26, [astro-ph/0601544].
 - [58] Sandage, A., *The Change of redshift and Apparent Luminosity of Galaxies due to the Deceleration of Selected Expanding Universes*, 1962, *ApJ* 136:319–333.
 - [59] Bolotin, Y. L., Erokhin, D. A., & Lemets, O. A. 2012, Physics Uspekhi, 55, A02
 - [60] Perlmutter, S., Aldering, G., Goldhaber, G., et al. 1999, ApJ, 517, 565
 - [61] Riess, A. G., Filippenko, A. V., Challis, P., et al. 1998, AJ, 116, 1009
 - [62] Barrow, J. D., Bean, R., & Magueijo, J. 2000, Mon. Non. Roy. Astron. Soc., 316, L41
 - [63] Li, Z., Wu, P., & Yu, H., "Examining the cosmic acceleration with the latest Union2 supernova data", 2011, Physics Letters B, 695, 1
 - [64] Shafieloo, A., Sahni, V., & Starobinsky, A. A., "Is cosmic acceleration slowing down?", 2009, Phys. Rev. D., 80, 101301
 - [65] Cárdenas, V. H., Bernal, C., & Bonilla, A., "Cosmic slowing down of acceleration using f_{gas} ", 2013, Mon. Non. Roy. Astron. Soc., 433, 3534
 - [66] Magaña, J., Motta, V., Cárdenas, V. H., & Foëx, G. 2017, Mon. Non. Roy. Astron. Soc., 469, 47
 - [67] Bonilla Rivera, A., & García Farieta, J., "Exploring the Dark Universe: Constraint on dynamical dark energy models from CMB, BAO and Growth Rate Measurements", 2016, arXiv:1605.01984
 - [68] Hu W., Sugiyama N., 1996, ApJ 471, 542
 - [69] Bond J. R., Efstathiou G., Tegmark M., 1997, MNRAS 291, L33

- [70] Eisenstein, D. J., Zehavi, I., Hogg, D. W., et al. 2005, ApJ, 633, 560
 [71] Percival W. J. et al., 2010, MNRAS, 401, 2148
 [72] Eisenstein D. J., Hu W., ApJ, **496**, 605 (1998)
 [73] Beutler, F., Blake, C., Colless, M., et al. 2011, Mon. Non. Roy. Astron. Soc., 416, 3017
 [74] Anderson L. et al., MNRAS **441**, 24 (2014).

Appendix A: Appendix A

1. β -model and triaxial ellipsoids

In the distribution described by an ellipsoidal triaxial β -model, the electron density of the intracluster gas is assumed to be constant on a family of similar, concentric, coaxial ellipsoids. In a coordinate system relative to GC, the electron density distribution is

$$n_e = n_{e0} \left(1 + \frac{\sum_{i=1}^3 v_i^2 x_{i,int}^2}{r_c^2} \right)^{-3\beta/2} \quad (\text{A1})$$

where $x_{i,int}$ is the intrinsic orthogonal coordinate system centred on GC's barycenter, r_c is characteristic length scale distribution at core radius, v_i is the inverse of the corresponding core core radius, n_{e0} is the central electron density. if we take the axial ratios $e_1 \equiv v_1/v_2$, $e_2 \equiv v_2/v_3$, $r_{c3} = r_c/v_3$ and and taking into account that

$$\frac{x}{a} + \frac{y}{b} + \frac{z}{c} = r_{ellp} \quad (\text{A2})$$

such that $x_1 = x$, $x_2 = y$, $x_3 = z$ and $v_1 = a^{-1}$, $v_2 = b^{-1}$, $v_3 = c^{-1}$ (see Fig. 4), we can obtain

$$n_e = n_{e0} \left(1 + \frac{e_1^2 x_{1,int}^2 + e_2^2 x_{2,int}^2 + x_{3,int}^2}{r_c^2} \right)^{-3\beta/2} \quad (\text{A3})$$

with

$$\beta = \frac{\nu m_p \sigma_v^2}{k_B T_e}. \quad (\text{A4})$$

Then the electron density distribution is described by five parameters in a ellipsoidal triaxial β -model: n_{e0} , β , e_1 , e_2 and r_{c3} .

The projection along the *los* of the electron density distribution, to a generic power m in the observer coordinate system is given by

$$\int_{los} n_e^m(l) dl = n_{e0}^m \sqrt{\pi} \frac{\Gamma(3m\beta - 1/2)}{\Gamma(3m\beta/2)} \frac{d_A \theta_3}{\sqrt{h}} \left(1 + \frac{\theta_1^2 + e_{proj}^2 \theta_2^2}{\theta_{c,proj}^2} \right)^{1/2 - 3\beta/2} \quad (\text{A5})$$

where d_A is the angular diameter distance in a *FRW* universe, $\theta_i \equiv x_{i,obs}/d_A$ e_{proj} is the projected angular position on the plane of the sky (*pos*) of the intrinsic orthogonal coordinate system $x_{i,obs}$ and h is a function of the GC shape and orientation:

$$h = e_1^2 \sin^2 \theta_{Eu} \sin^2 \varphi_{Eu} + e_2^2 \sin^2 \theta_{Eu} \cos^2 \varphi_{Eu} + \cos^2 \theta_{Eu}, \quad (\text{A6})$$

such that θ_{Eu} and φ_{Eu} are the Euler angles in the GC coordinate system (see Fig. 4) and

$$\theta_{c,proj} \equiv \theta_{c3} \left(\frac{e_{proj}}{e_1 e_2} \right)^{1/2} h^{1/4}. \quad (\text{A7})$$

If we assume that the intracluster medium is described by an isothermal triaxial β -model distribution with $m=1$ we obtain

$$\Delta T_{sz} = \Delta T_{sz0} \left(1 + \frac{\theta_1^2 + e_{proj}^2 \theta_2^2}{\theta_{c,proj}^2} \right)^{1/2-3\beta/2} \quad (A8)$$

where ΔT_{sz0} is the central temperature decrement of SZ effect, which is given by

$$\Delta T_{sz0} \equiv T_{cmb} f(\nu, T_e) \frac{k_B T_e}{m_e c^2} n_{e0} \sqrt{\pi} \frac{d_A \theta_{c,proj}}{h^{4/3}} \sqrt{\frac{e_1 e_2}{e_{proj}}} g\left(\frac{\beta}{2}\right) \quad (A9)$$

and

$$g(\alpha) \equiv \frac{\Gamma(3\alpha - 1/2)}{\Gamma(3\alpha)}. \quad (A10)$$

e_{proj} is the axial ratio of the major to minor axes of the observed projected isophotes and $\theta_{c,proj}$ is the projection on the (pos).

On the other hand, the X-Ray surface brightness for intracluster medium with $m=2$, is given by

$$S_x = S_{x0} \left(1 + \frac{\theta_1^2 + e_{proj}^2 \theta_2^2}{\theta_{c,proj}^2} \right)^{1/2-3\beta/2} \quad (A11)$$

where the central surface brightness S_{x0} is

$$S_{x0} \equiv \frac{\Lambda_{eH}(\mu_e/\mu_H)}{4\sqrt{\pi}(1+z)^4} n_{e0} \frac{d_A \theta_{c,proj}}{h^{4/3}} \sqrt{\frac{e_1 e_2}{e_{proj}}} g(\beta), \quad (A12)$$

with $\mu_i \equiv \rho/(n_i m_p)$ the molecular weight.

2. Galaxy clusters data

Table VIII shows us the experimental cosmological distance with triaxial symmetry from De Filippis et al. obtained by the method S-Z/X-Ray [1]. Column 1 shows the cluster identification name, column 2 give the correspond redshift, column 3 is gas temperature, column 4 is central temperature decrement, column 5 is the term of dependence with frequency with relativistic corrections and column 6 show us the experimental cosmological distance. Fig 5. show us the angular diameter distance vs reshift and the data sample from De Filippis et al.

Appendix B: Appendix B

1. SNIa

Here, we use the Union 2.1 sample which contains 580 data points. The SNIa data give the luminosity distance through the relation $d_L(z) = (1+z)^2 d_A(z)$. We fit the SNIa with the cosmological model by minimizing the χ^2 value defined by

$$\chi_{SNIa}^2 = A - \frac{B^2}{C} \quad (B1)$$

where

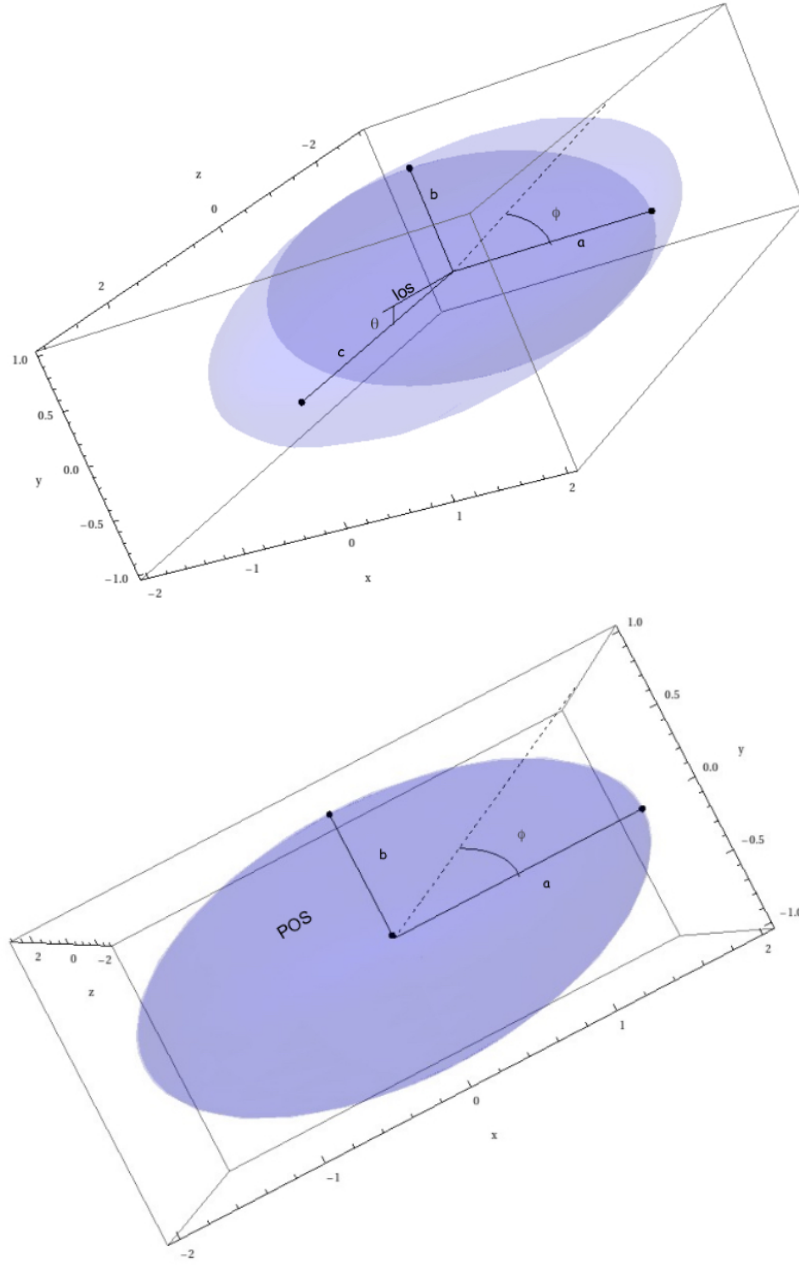


FIG. 4: Ellipsoid coefficients a , b and c , with the *los* making an angle θ with the z -axis (up). View of the *pos* with the *los* oriented along the z -axis (down).

$$A = \sum_{i=1}^{580} \frac{[\mu_{th}(z_i, p_i) - \mu_{obs}(z_i)]^2}{\sigma_{\mu_i}^2},$$

$$B = \sum_{i=1}^{580} \frac{\mu_{th}(z_i, p_i) - \mu_{obs}(z_i)}{\sigma_{\mu_i}^2}, \quad (B2)$$

Cluster	z_i	$k_B T_e$ (keV)	ΔT_{sz0} (μK)	$f(\nu, T_e)$	$D_c _{exp}^{ell}$ (Mpc)
MS 1137.5+6625	0.784	$5.7^{+1.3}_{-0.7}$	-818^{+98}_{-113}	2.00	2479 ± 1023
MS 0451.6-0305	0.550	$10.4^{+1.0}_{-0.8}$	-1431^{+98}_{-105}	1.87	1073 ± 238
Cl 0016+1609	0.546	$7.55^{+0.72}_{-0.58}$	-1242 ± 105	1.89	1635 ± 391
RXJ1347.5-1145	0.451	$9.3^{+0.7}_{-0.6}$	-3950 ± 350	1.91	1166 ± 262
A 370	0.374	$6.6^{+0.7}_{-0.5}$	-785 ± 118	1.96	1231 ± 441
MS 1358.4+6245	0.327	$7.48^{+0.50}_{-0.42}$	-784 ± 90	1.88	697 ± 183
A 1995	0.322	$8.59^{+0.86}_{-0.67}$	-1023^{+83}_{-77}	1.91	885 ± 207
A 611	0.288	6.6 ± 0.6	-853^{+120}_{-140}	1.76	934 ± 331
A 697	0.282	9.8 ± 0.7	-1410^{+160}_{-180}	1.89	1099 ± 308
A 1835	0.252	$8.21^{+0.19}_{-0.17}$	-2502^{+150}_{-175}	1.93	946 ± 131
A 2261	0.224	$8.82^{+0.37}_{-0.32}$	-1697 ± 200	1.87	1118 ± 283
A 773	0.216	$9.29^{+0.41}_{-0.36}$	-1260 ± 160	1.76	1465 ± 407
A 2163	0.202	$12.2^{+1.1}_{-0.7}$	-1900 ± 140	1.90	806 ± 163
A 520	0.202	$8.33^{+0.46}_{-0.40}$	-662 ± 95	1.93	387 ± 141
A 1689	0.183	$9.66^{+0.22}_{-0.20}$	-1729^{+105}_{-120}	1.86	604 ± 84
A 665	0.182	$9.03^{+0.35}_{-0.31}$	-728 ± 150	1.87	451 ± 189
A 2218	0.171	$7.05^{+0.22}_{-0.21}$	-731^{+125}_{-100}	1.95	809 ± 263
A 1413	0.142	$7.54^{+0.17}_{-0.16}$	-856 ± 110	1.88	478 ± 126
A 2142	0.091	7.0 ± 0.2	-437 ± 25	1.87	335 ± 70
A 478	0.088	8.0 ± 0.2	-375 ± 28	1.91	448 ± 185
A 1651	0.084	8.4 ± 0.7	-247 ± 30	1.75	749 ± 385
A 401	0.074	6.4 ± 0.2	-338 ± 20	1.78	369 ± 62
A 399	0.072	9.1 ± 0.4	-164 ± 21	1.81	165 ± 45
A 2256	0.058	9.7 ± 0.8	-243 ± 29	1.96	242 ± 61
A 1656	0.023	6.6 ± 0.2	-302 ± 48	1.96	103 ± 42

TABLE VIII: Galaxy Cluste data set from De Filippis et al. for 25 data point (S-Z/X-Ray) [1].

$$C = \sum_{i=1}^{580} \frac{1}{\sigma_{\mu_i}^2},$$

where $\mu(z) \equiv 5 \log_{10}[d_L(z)/\text{Mpc}] + 25$ is the theoretical value of the distance modulus, and we have marginalized over the nuisance parameter μ_0 and μ_{obs} .

2. CMB

A particular cosmological test to probe dark energy is the angular scale of sound horizon (r_s) at time of decoupling ($z_{cmb} \sim 1090$), the which is encrypted in the location l_1^{TT} of the first peak of the CMB power spectrum. We include CMB information of Planck 13 data [29] to probe the expansion history up to the last scattering surface. The χ^2 for the CMB data is constructed as

$$\chi_{CMB}^2 = X_{Planck13}^T C_{cmb}^{-1} X_{Planck13}, \quad (B3)$$

such that

$$X_{Planck13} = \begin{pmatrix} l_A - 301.57 \\ R - 1.7407 \\ \omega_b - 0.02228 \end{pmatrix}, \quad (B4)$$

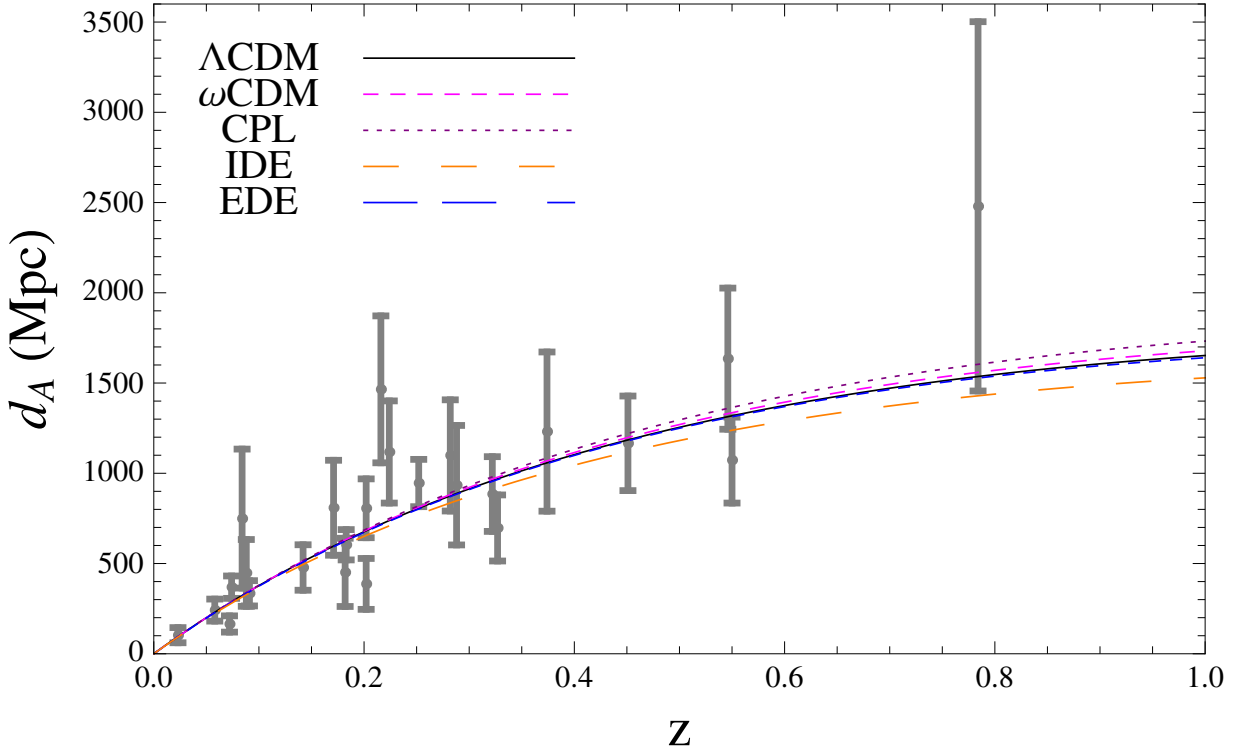


FIG. 5: Angular diameter distance vs redshift for different models with the best fit values from joint analysis (CMB+BAO+SNIa+ d_A + f_{gass} +SGL) and 25 data set from De Filippis et al. (Gray) [1].

where $\omega_b = \Omega_b h^2$. Here l_A is the "acoustic scale" defined as

$$l_A = \frac{\pi d_A(z_{cmb})(1 + z_{cmb})}{r_s(z_{cmb})}, \quad (B5)$$

where $d_A(z_{cmb})$ is the angular diameter distance and z_{cmb} is the redshift of decoupling given by [68],

$$z_{cmb} = 1048[1 + 0.00124(\Omega_b h^2)^{-0.738}][1 + g_1(\Omega_m h^2)^{g_2}], \quad (B6)$$

$$g_1 = \frac{0.0783(\Omega_b h^2)^{-0.238}}{1 + 39.5(\Omega_b h^2)^{0.763}}, g_2 = \frac{0.560}{1 + 21.1(\Omega_b h^2)^{1.81}}, \quad (B7)$$

The "shift parameter" R is defined as [69]

$$R = \frac{\sqrt{\Omega_m}}{c} d_A(z_{cmb})(1 + z_{cmb}). \quad (B8)$$

C_{cmb}^{-1} in Eq. (B3) is inverse covariance matrix for (R, l_A, ω_b) , which to Planck 13 data is:

$$C_{cmbPlanck13}^{-1} = \sigma_i \sigma_j C_{NorCov_{i,j}}, \quad (B9)$$

where $\sigma_i = (0.18, 0.0094, 0.00030)$ and normalized covariance matrix is:

$$C_{NorCov_{i,j}} = \begin{pmatrix} 1.0000 & 0.5250 & -0.4235 \\ 0.5250 & 1.0000 & -0.6925 \\ -0.4235 & -0.6925 & 1.0000 \end{pmatrix}. \quad (B10)$$

This test contributes with 3 data points to the statistical analysis.

3. BAO

The large scale correlation function measured from SDSS, includes a peak which was identified with the expanding spherical wave of baryonic perturbations from acoustic oscillations at recombination and comoving scale of about $150Mpc$. The expected BAO scale depends on the scale of the sound horizon at recombination and on transverse and radial scales at the mean redshift of galaxies in the survey. For obtain constraints on cosmological model we begin with χ^2 for WiggleZ BAO data [32], which is given by

$$\chi_{WiggleZ}^2 = (\bar{A}_{obs} - \bar{A}_{th}) C_{WiggleZ}^{-1} (\bar{A}_{obs} - \bar{A}_{th})^T, \quad (B11)$$

where $\bar{A}_{obs} = (0.447, 0.442, 0.424)$ is data vector at $z = (0.44, 0.60, 0.73)$ and $\bar{A}_{th}(z, p_i)$ is given by [70]

$$\bar{A}_{th} = D_V(z) \frac{\sqrt{\Omega_m H_0^2}}{cz}, \quad (B12)$$

in which $D_V(z)$ is the distance scale defined as

$$D_V(z) = \frac{1}{H_0} \left[(1+z)^2 d_A(z)^2 \frac{cz}{E(z)} \right]^{1/3}. \quad (B13)$$

Here, $d_A(z)$ is the angular diameter distance. Additionally, $C_{WiggleZ}^{-1}$ is the inverse covariance matrix for the WiggleZ data set given by

$$C_{WiggleZ}^{-1} = \begin{pmatrix} 1040.3 & -807.5 & 336.8 \\ -807.5 & 3720.3 & -1551.9 \\ 336.8 & -1551.9 & 2914.9 \end{pmatrix}. \quad (B14)$$

Similarly, for the SDSS DR7 BAO distance measurements, χ^2 can be expressed as [71]

$$\chi_{SDSS}^2 = (\bar{d}_{obs} - \bar{d}_{th}) C_{SDSS}^{-1} (\bar{d}_{obs} - \bar{d}_{th})^T, \quad (B15)$$

where $\bar{d}_{obs} = (0.1905, 0.1097)$ is the data points at $z = 0.2$ and $z = 0.35$. Here, $\bar{d}_{th}(z_d, p_i)$ denotes the distance ratio

$$\bar{d}_{th} = \frac{r_s(z_d)}{D_V(z)}, \quad (B16)$$

in which $r_s(z)$ is the comoving sound horizon given by

$$r_s(z) = c \int_z^\infty \frac{c_s(z')}{H(z')} dz', \quad (B17)$$

and $c_s(z)$ is the sound speed

$$c_s(z) = \frac{1}{\sqrt{3(1 + \bar{R}_b/(1+z))}}, \quad (B18)$$

with $\bar{R}_b = 31500 \Omega_b h^2 (T_{CMB}/2.7K)^{-4}$ and $T_{CMB} = 2.726K$. The redshift z_{drag} at the baryon drag epoch is fitted with the formula proposed in [72],

$$z_{drag} = \frac{1291(\Omega_m h^2)^{0.251}}{1 + 0.659(\Omega_m h^2)^{0.828}} [1 + b_1(\Omega_b h^2)^{b_2}], \quad (B19)$$

where

$$b_1 = 0.313(\Omega_m h^2)^{-0.419}[1 + 0.607(\Omega_m h^2)^{0.674}] \quad (\text{B20})$$

and

$$b_2 = 0.238(\Omega_m h^2)^{0.223}. \quad (\text{B21})$$

Here C_{SDSS}^{-1} is the inverse covariance matrix for the SDSS data set given by

$$C_{SDSS}^{-1} = \begin{pmatrix} 30124 & -17227 \\ -17227 & 86977 \end{pmatrix}. \quad (\text{B22})$$

For the 6dFGS BAO data [73], there is only one data point at $z = 0.106$, the χ^2 is easy to compute

$$\chi_{6dFGS}^2 = \left(\frac{d_z - 0.336}{0.015} \right)^2. \quad (\text{B23})$$

The total χ^2 for all the BAO data sets thus can be written as

$$\chi_{BAO}^2 = \chi_{BW}^2 + \chi_{SDSS}^2 + \chi_{6dFGS}^2. \quad (\text{B24})$$

Additionally, we include measures from the Main Galaxy Sample of Data Release 7 of Sloan Digital Sky Survey (SDSS-MGS) [74] $r_s/D_V(0.57) = 0.0732 \pm 0.0012$. Then, the total χ_{BAO}^2 is given by

$$\chi_{BAO}^2 = \chi_{WiggleZ}^2 + \chi_{SDSS}^2 + \chi_{6dFGS}^2 + \chi_{SDSS-MGS}^2 \quad (\text{B25})$$